Synthesis of TiO_2/Pd/Multi-Walled Carbon Nano-Structures by Hydrothermal Technique and deposited it on n-Si substrate as TiO_2/Pd/MWCNTs:n-Si Heterojunction by Pulsed Laser Deposition

The 5th International scientific Conference on Nanotechnology& Advanced Materials Their Applications (ICNAMA 2015) 3-4 Nov, 2015

Dr .Saif M. Alshrefi
College of Science for Women , Babylon University/ Babylon.
Email: Saif_master80@yahoo.com
Dr.Dunia K. Mahdi
College of Science ,Baghdad University/ Baghdad.
Dr.Zainab S. Sadik
College of Science ,Baghdad University/Baghdad.

Abstract

Carbon nanostructures (CNTs) have been prepared by a Hydrothermal deposition technique based on the polymer Polyethylene glycol (PEG) dissolved in water and Ethanol alcohol of a new carbon sources materials mixed with ($PdCl_2$) as a catalyst mixed with Sodium hydroxide (8gm NaOH) using Parr reactor at temperature (190°C) and forming the hybrid composite material (TiO_2/Pd/MWCNTs) by the same way. Thence, deposited heterojunction material (TiO_2/Pd/MWCNTs:n-Si) using the Pulsed Laser Deposition Technique (PLD), on the substrate of n-silicon wafer. The obtained (MWCNTs & TiO_2/Pd/MWCNTs) are investigated by scanning electron microscope (SEM), X-ray diffraction (XRD) and X-ray Photo-electron Spectroscopy (XPS). Normal MWCNTs are formed multi-walled carbon nanotubes (MWCNTs) and carbon nanosheets (CNSs) but in little bit amount. MWCNTs were obtained as main products with lengths of (1.6–3 μm) and diameters of (30-60 nm) could be synthesized at as low temperature as (190°C). Deconvolution of the (C1s) peaks which characteristic of C-C bonds, showed a main peak at (284.96 and 285.04 eV) with total amount (74.96 and 30.64 at%) for the product of MWCNTs and TiO_2/Pd/MWCNTs composite respectively. Current – voltage characteristics of heterojunction showed that forward bias current change exponentially approximately with applied voltage at dark and this agreement with tunneling–recombination model. Also (I-V) characteristics under illumination of TiO_2/Pd/MWCNTs heterojunction deposited on p-Si substrate (η=10.5) efficiency in Solar Cell.

Keyword: Carbon Nanotubes, Hybrid Materials, Hydrothermal Technique, Pulsed Laser Deposition (PLD).

توليف المادة المركبة ثنائي اوكسيد التيتانيوم/البلاديوم/مركبات الكاربون النانوية المتعددة الجدران بطريقة الهايدرو حراري وترسيبها على شرائح السليكون السالبة لتكوين المفرق المهجن بطريقة الترسيب بالليزر النبضي

الخلاصة:

تم تحضير الكاربون النانوي المتعدد الأشكال باستخدام تقنية الهايدرو حراري (Hydrothermal Technique) المعتمدة على البوليمر (بولي إيثيلين كلايكول-PEG) المضاف إلى الماء وكحول

https://doi.org/10.30684/etj.33.5B.12
2412-0758/University of Technology-Iraq, Baghdad, Iraq

الإيثانول كمصدر آخر للكاربون مخلوطاً مع محفز للتفاعل وهو ($PdCl_2$) و (8gm) من هيدروكسيد الصوديوم مع نقل المواد المتفاعلة إلى داخل عبوة مصنوعة من الستيل عالي الضغط ومحكمة الإغلاق وبواسطة محفز أو عامل مساعد للتفاعل عند درجة حرارة (190ºC) اضافة الى تكوين المادة المتراكبة (TiO_2/Pd/MWCNTs) بواسطة نفس التقنية. عندئذ تم ترسيب أغشية المفرق المهجن (TiO_2/Pd/MWCNTs:n-Si) بواسطة تقنية الترسيب بالليزر النبضي على قواعد من السليكون . دُرستْ خواص كل من المواد (الكاربون النانوب الانبوبي والمادة المتراكبة MWCNTs &) (TiO_2/Pd/MWCNTs) بواسطة المجهر الالكتروني الماسح وحيود الأشعة السينية وفحص (XPS) . أظهر فحص المجهر الإلكتروني الماسح تكوّن أشكال الكاربون (ألأنابيب ، الصفائح لكن بكمية قليلة) بأطوال (1.6–3 μm) و بمعدل (30-60 nm) لقطر الأنبوب الكاربوني النانوي . كما أظهر فحص (XPS) عند تحليل مكونات العينات أن قمم اوربيتال الكاربون (C1s) للآصرة (C-C) كانت عند طاقة الربط (284.96 eV) و (285.04 eV) وبمحتوى كلي (74.93 at%) و (30.64 at%) لمنتج MWCNTs وللمادة المتراكبة TiO_2/Pd/MWCNTs على التوالي . بينت قياسات تيار – جهد إن تيار الانحياز الأمامي عند الظلام يتغير تقريبا اسياً مع الفولتية المسلطة و المفرق تتطابق مع نموذج إعادة الاتحاد- انتفاق. وكذلك بينت قياسات التيار – جهد عند الإضاءة إن المفارق المهجنة المحضرة من أغشية (TiO_2/Pd/MWCNTs) عند درجة حرارة الغرفة على أساس من n-Si تكون ذات كفاءة جيدة وأفضلها عند النسبة (10.5 %) .

الكلمات المفتاحية: الكاربون الأنبوبي النانوي وأشكاله ، المواد المتراكبة ، تقنية الهايدرو حراري ، تقنية الترسيب بالليزر النبضي .

INTRODUCTION

Ever since the discovery of fullerene in 1985[1] and carbon nanotubes (CNTs) in 1991[2], carbon nanoscale materials have been reported to be very attractive candidates. Various forms of carbon nanomaterials have been reported such as fullerenes [1], carbon nanotubes (single-walled and multi-walled) [2,3], carbon nanofibres [4], carbon nanohorns [5], carbon nanocapsules[6], carbon nano-onions[7], carbon nanospheres[8], helical carbon nanotubes (HMWCNTs) [9], ferromagnetic-filled carbon nanotubes[10] and carbon nanosheets[11]. Due to their unusual properties, a wide variety of scientific and technological research has been focused on the use of nanocarbons, in terms of their potential applications as well as their large scale synthesis. For the production of nanocarbons, there exist several techniques such as arc discharge[2,3], laser vaporization [1], hydrocarbon pyrolysis [12], high-pressure catalytic decomposition of carbon monoxide (HiPCO) [13], pyrolysis [14,15], flame synthesis [13], chemical vapor deposition(CVD)[16], plasma-enhanced CVD (PECVD)[17], electrophoretic deposition (EPD)[17] and Hydrothermal technique[18],etc. Each and every synthesis method is related with obtaining adequate active atomic carbon species or clusters from the carbon source materials and assembles them into nanocarbons in the presence of or without catalyst. The advantage of liquid hydrocarbons as carbon source materials is that they are cheaper and controlled insertion of liquid additive can be introduced into the reactor where they form active carbon species for carbon nanostructure's growth. Size as well as type of catalysts affects the morphology and yield of carbon nanotubes. In general, catalyst particles were obtained by decomposing organometallic precursors. However, considering the toxicity of the organometallics, a safer method of producing catalyst in situ is still needed. There have been intensive efforts in

exploring innovated solar cell structures with high performance and cost-effective manufacturing methods molecules (with efficiencies of 7%)[19,20]. Emerging competitive technologies include solar cells based on organic[21,22], colloidal quantum dots (efficiencies reaching 6%)[23,24], and dye-sensitized solar cells (efficiencies up to 12%)[25-27]. An alternative approach is to combine inexpensive materials with well-established semiconductors (e.g. silicon) to create new architectures that have the potential of simplifying fabrication processes and lowering cost. To this end, researchers have explored various candidates, particularly transparent conductive films of carbon nanotubes (CNTs), graphene and semiconducting polymers that can be conveniently deposited on commercial Si wafers to make efficient solar cells[28–36]. During the past years, considerable progresses have been achieved in this area and power conversion efficiencies have been steadily enhanced to about 8% for graphene-Si[37] and 13.8% for acid-doped CNT-Si cells[31]. Antireflection structures such as vertical semiconducting nanowire arrays grown on or etched from a Si substrate[38], nanodome-like amorphous Si films[39], and patterned Si nanocones[18] with suitable aspect ratios have been reported recently, and showed effective light trapping and reflection reduction for the devices. Those approaches generally created a rough surface on top of the Si substrate and involved complex photolithography techniques to make patterns. In addition, the non-smooth Si surface may prevent conformal transfer of nanotube or graphene films and bring additional charge recombination sites, for example, on the surface of patterned nanowires and nanocones. Recently, several groups and our team have particularly studied CNT-silicon solar cells that were fabricated by transferring a semi-transparent CNT film onto a n-type single-crystalline Si wafer and heterojunctions[28–33,40].

Materials and Method

Experimentally, the product of carbon nano-structures manufactured at first by Hydrothermal Technique, prepare TiO_2/Pd-MWCNTs composite secondly by Hydrothermal Technique as well, then pressing the powder of TiO_2/Pd/MWCNTs heterojunction and transfer it to Pulsed Laser Deposition system to prepare (TiO_2/Pd/MWCNTs:n-Si) substrates.

Synthesis of MWCNTs: In this synthesis, (80 ml) Ethyl alcohol, (20 ml) water, (8gm) NaOH and (4gm) Polyethylene glycol (PEG-20.000Mw $(C_2H_4O)_{n+1}H_2O)$) supported from (VWR Company), were added to a (250 ml) flask. The chemicals were transferred to magnetic stirrer for (30 min). Then, Palladium chloride (0.1 gm $PdCl_2$) dissolved in (15 ml) water as a catalyst, which still in a magnetic stirrer for (1 hr.), all of chemicals mixed in (200 ml) Teflon Jar and interblended in a magnetic stirrer for (45 min). Finally, transferred to a Parr reactor (Home made which modify Series 5500 High Pressure Compact Parr Reactor Model, in Georgia Institute of Technology-MSE, Georgia, USA) as in figure(1), with a capacity of (250 ml). The Parr reactor was sealed and then kept at (190 ºC for 24 hr.) in a furnace, then cooled down to room temperature, wash the product with alcohol and water for five times. Finally, dried in a vacuum oven at (70 ºC) for (10 hr.).

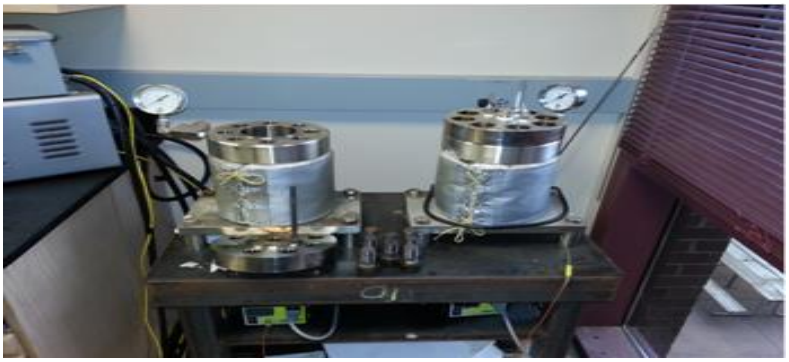

Figure (1) Parr Reactor Autoclave (Home made).

Manufacturing of TiO_2/Pd/MWCNTs Composite: Titanium Oxide (TiO_2) and Palladium nanoparticles can be hybrid with (MWCNTs) by hydrothermal method. The hybrid (doped) set of samples with (TiO_2) & ($PdCl_2$) had been dissolving two solutions. The first one, resolve (3 gm of NaOH) in (10 ml of water) and prepare stirred solution of (3gm of TiO_2 (grain size:30-40 nm)) dispersed in (30ml water), beside the second one, (0.1 gm) of $PdCl_2$ dissolved in (10 ml) of water then mixed all the solutions to transfer them to the Autoclave for (24 hr.) under a temperature of (190°C) with immerse Piece of High carbon steel (3cm, 1.5cm, 0.4cm) as in figure (2), inside Teffelon Jar of the Autoclave in order to increase the encouraging combined TiO_2 with MWCNTs. Switch off the autoclave and leave it cool down at room temperature. The product powder was washed with alcohol and water well for 5 times and dried at (70 °C) for (24 hr.).

Figure (2) Schematic of Piece of steel inside the Autoclave.

Preparation of (TiO_2/Pd/MWCNTs:n-Si) Substrates by Pulsed Laser Deposition System

The Nd:YAG Laser system (Q-Switched Nd:YAG Laser MED-810 Beijing KES Biology Technology Co.Ltd.) with wavelength (1064 nm), which enabled quality factor of a repetitive rate (6 Hz), pulse duration (10 ns) and laser energy (1000 mJ) on the substrate of n-silicon wafer. This system is compact and allows controlling the main parameters by a computer system, such as power and repetition rate. PLD

system contains of three major components which are vacuum chamber, vacuum pumps and vacuum gauges.

Thin films in nano-scales prepared by PLD system, consists of the main parts shown in figure (3): vacuum chamber, Q- switched Nd:YAG Laser**,** lens with focal length (30) cm**,** quartz window, pressure monitoring**,** rotary pump, diffusion pump and Ar gas cylinder.

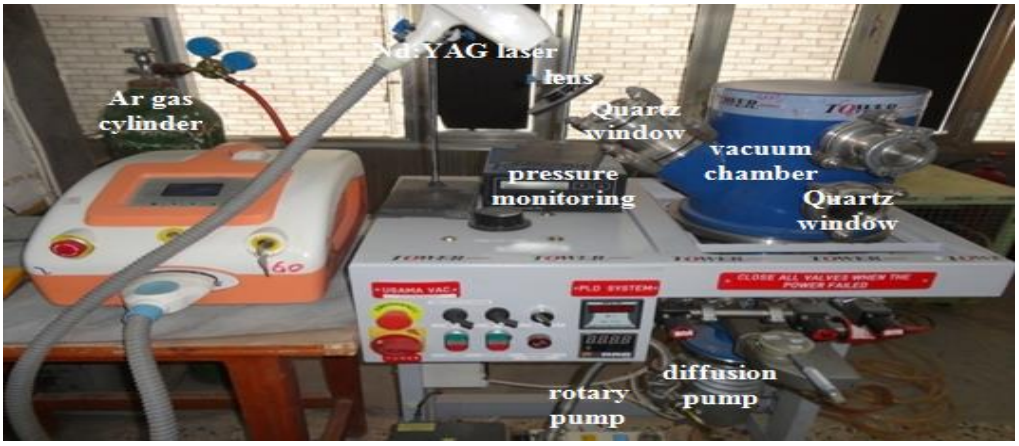

Figure (3) PLD system Set-Up.

Results and Discussion

As shown in figure (4) a, it became carbon in its various forms is a precipitate formed brown and black color because of the cofactors of the reaction, which created a suitable environment for the growth of carbon structures by the role of Palladium chloride, which represents a new role for these two factors in determining the color of the emulsion dark brown and very thick by hydrothermal technique, This preliminary result, consistent with the findings of the other researchers[41,42,43]. The important thing is used ($PdCl_2$) as a catalyst to synthesized MWCNTs, after that synthesized Pd NPs to hybrid material now. As shown from figure (5), the appearance of semi-spherical structures of large size is a MWCNTs with palladium, their have coverage entirely by TiO_2 (confirmed by XPS later). Note that piece of steel inside teffelon jar has completely covered with TiO_2 and Pd/MWCNTs, which attract ingredients floating in solution. The ingredients collected well and slide to the bottom, and stable last components of the reaction solution on piece of High carbon steel. This shows the role of the elements within the piece of High carbon steel which are iron, nickel and cobalt created a compromise suitable to connect the components in the reaction solution. In figure (6-a) show the FE-SEM images (Zeiss ULTRA 60 FE-SEM, at the Georgia Tech./MSE.-USA) of the as-synthesized MWCNTs.

Figure (4) Images of resulting emulsion of preparation.

Figure (5) Image of product for TiO_2/Pd/MWCNTs after removing it from autoclave directly.

It is worth pointing out that the diameters of the as-prepared MWCNTs by the current low-temperature hydrothermal route are much smaller than those prepared by high-temperature hydrothermal method[12]. The length of the MWCNTs is (1.6–3 μm) and diameters of (30-60 nm). From the point of view of chemistry, the compound is stable and by Le Chatelier's principle. which if a chemical system at equilibrium experiences a change in concentration, temperature, volume, or pressure, then the equilibrium shifts to counteract the imposed change and a new equilibrium is established, then will disintegrate chemical compound $C_2H_5O^-$ Na^+ to $C_2H_5O^-$ and Na^+, when it is mixed with the PEG presence of heat and pressure will produce the chemical compound, this case is called polymerization. It is a process of reacting monomer molecules together in a chemical reaction to form polymer chains or three-dimensional networks.

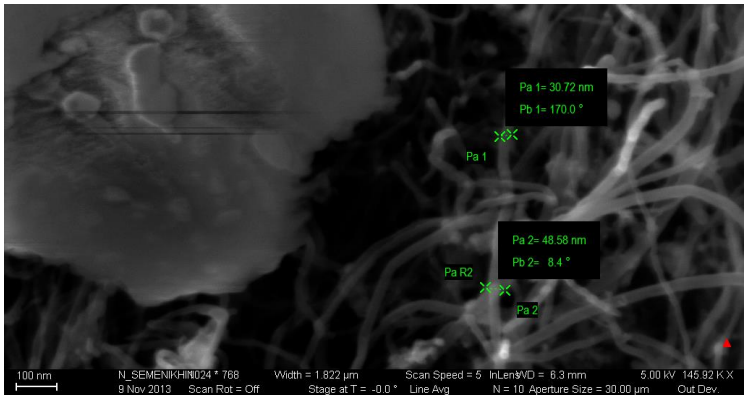

(a)

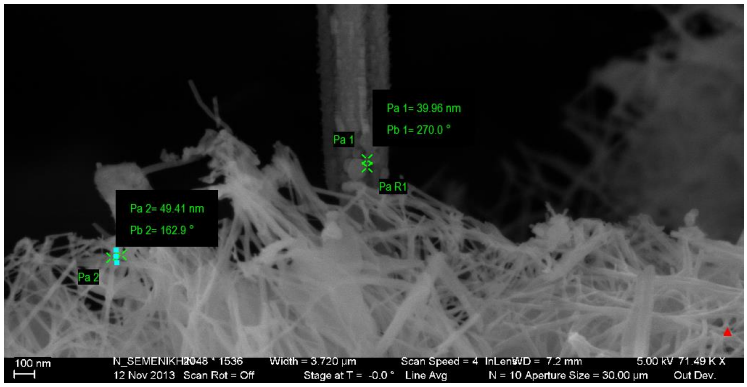

(b)

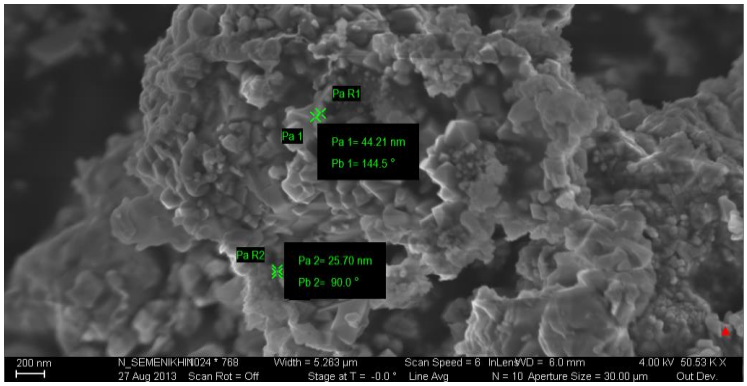

(c)

Figure (6) FE-SEM images of: a/ MWCNTs; b/ TiO_2-$PdCl_2$; c/ (Hybrid – TiO_2/Pd/MWCNTs).

So, OH^- with $C_2H_5O^-$will replaced due to the high temperature and pressure and will be formed Etheric bond because the beginning of the interaction. There for, the required time is not enough to produce chain of MWCNTs or MWCNTs, but important thing is the increase in temperature leads to an increase of particle size and then in the small surface area and thus less efficient product. Figure (6-b) shows the

the FE-SEM image of TiO_2 and Pd NPs. The interface connection between Pd and TiO_2 can clearly be observed, indicating that TiO_2 nanoparticles were well attached on the surface of $PdCl_2$. Figure (6-c) shows the FE-SEM image of the TiO_2/Pd/ MWCNTs. Illegible porous structures in the TiO_2 nanoparticles can be observed, which may contribute to a high specific surface area. Some TiO_2 and Pd nanoparticles were intimately bound to the surface of TiO_2/Pd/ MWCNTs. MWCNTs in the hybrid material had intimate contact with TiO_2 nanoparticles, the diameter of the coated MWCNTs significantly increases and consequently the inner core of MWCNTs is hardly visible. In addition to that, well-dispersed MWCNTs in the hybrid material had intimate contact with TiO_2 nanoparticles, which possess a particle diameter in the range of (36–44 nm), and (20-42 nm) for Pd with mean particle size (36.30-43.53 nm) for TiO_2/Pd/ MWCNTs. and average value (36 nm) for Pd. Owing to the presence of MWCNTs which reduced the self-agglomeration of TiO_2 NPs by restricting its direct contact. The particle size of TiO_2 is moderately decreased with the increasing content of MWCNTs in the hybrid, owing to the presence of MWCNTs which reduced the self-agglomeration of TiO_2 nanoparticles by restricting its direct contact. The X-ray diffraction pattern (XRD) of the product was determined on X-ray diffractometer equipped with graphite monochromatized Cu-Ka radiation as in figure (7). The peaks can be indexed to (1 1 1) and (2 0 0) reflections of cubic close-packed Pd and the other peak at 26.5º can be indexed to (0 0 2) reflection of graphene layers. The above results confirm the reduction reaction of sodium hydroxide to sodium and disintegrate chemical compound $C_2H_5O^-$ Na^+ to $C_2H_5O^-$ and Na^+, when it is mixed with the PEG presence of heat and pressure will produce the chemical compound, this case is called polymerization, which occurs according to our design. According to XRD pattern, it exhibits a pair of small but strong peaks for (0 0 2) which indicates that [0 0 1] is the radial direction of carbon nanotubes and it indicate grown from the catalytic particles[12,15,18,20,21].The TiO_2/Pd/MWCNTs nanoparticles were of homogeneous anatase structure with crystallinity, and the average crystallite sizes calculated from Scherrer's equation (**$D= 0.9\lambda / \beta \cos\theta$** where: D is the crystallite size of the particles, λ is the x-ray wavelength used which is equal to 1.5406 A˚, β is the half-peak width for Pd (111) (as an example) in radian, $\cos\theta$ is the maximum angle of the (111) peak) were found to be about (36.96-43.53 nm). The two peak at $2\theta = 25.9°$ cannot be found easy and clearly in the TiO_2 NPs-coated MWCNTs except the two weak peak at $2\theta = 43.2°$. This is because the main peak of MWCNTs at $2\theta = 26.8°$ is overlapped by that of Anatase-TiO_2 at $2\theta = 25.2°$.

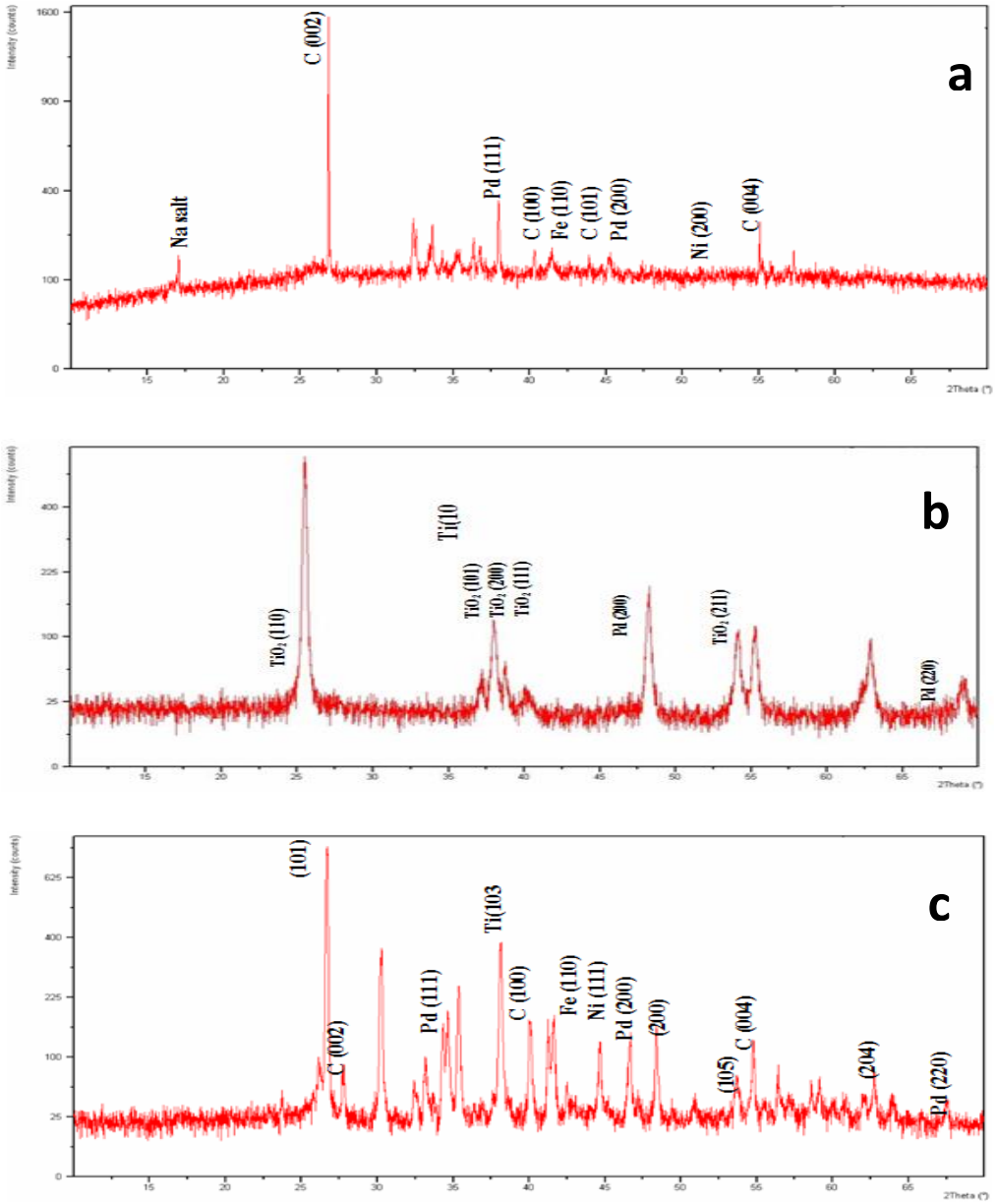

Figure (7) XRD pattern of : a- Carbon Nano-Structures (MWCNTs), b- TiO_2/Pd c- TiO_2/Pd/MWCNTs hybrid.

XPS is one of the surface analytical techniues, which can provide useful information on the nature of the functional groups and also on the presence of structural defects on the nanotube surface. Highly oxidative environment are associated with chemical shift. Calculations have also suggested that the oxidation rates of MWCNTs depend on the helical conformation of the nanotubes or nano sheets or nanofiber. Moreover, surface to core level shift (SCLS) phenomena is likely in functionalized multi-wall nanotubes. The survey peaks deconvolution of in figures

(8) & (9), deconvolution of MWCNTs and TiO_2/Pd/MWCNTs composite respectively. The (C1s) peaks which characteristic of C-C bonds, showed a main peak at (284.96 and 285.04 eV) with total amount (74.96 and 30.64 at%) for the product of MWCNTs and TiO_2/Pd/MWCNTs composite respectively, attributed to the graphitic structure in agreement with recent photoemission studies on MWCNTs [109,134] and defects on the nanostructures (tubes, sheets, fibers) [23,24], whereas the p–p* transition loss peak was detected at (290.40 eV), correspond to carbon atoms attached to different oxygen-containing moieties[23,24,25]. Deconvolution is complicated by the presence of different species (e.g., C-H, C-O, C=O,COOH) with similar binding energies. For MWCNTs, spectral deconvolution of the C(1s) region is further complicated by the presence of a π-π* shake-up feature that must be taken into account. Furthermore, XPS peak fitting cannot be used to distinguish between oxygen-containing functional groups which have the same binding energy (e.g., alcohols, C-OH vs. ethers, C-O-C). Deconvolution of the XPS O1s peak confirmed the presence of some carboxylic and hydroxyl functions onto the MWCNTs surface at (531.73 and 530.28 eV) with total amount (8.63 and 39.52 at.%) for the product of MWCNTs and TiO_2/Pd/MWCNTs composite respectively. Furthermore, oxygen related to the TiO_2 catalyst and NaOH. The XPS Na1s peak positions at (1072.18 and 1071.18 eV) with total amount (4.76 and 14.59 at%) for the product of MWCNTs and TiO_2/Pd/MWCNTs composite respectively. The presence of these peaks confirmed the presence of hydroxide a lot in two mixtures and physically adsorbed oxygen/carbonates were detected at (531.73 eV) with (8.63 at.%). So, it can be concluded that the impurity of MWCNTs includes the catalyst particles and graphitic platelets which amounts to about (17-20 at.%). As for the presence of both Cl2p and Pd3d in two mixtures that is due to using $PdCl_2$ as a catalyst. When dissolving $PdCl_2$ in water will get on Pd^+, and OH^-, this meaning presence of free Pd^+ ions in solution and with acid molecules 2HCl. Deconvolution of the XPS Cl2p peaks at (199.13 and 199.1 eV) with total amount (2.71 and 0.13 At%) for the product of MWCNTs and TiO_2/Pd/MWCNTs composite respectively, that confirmed it is individual chlorine related with another element not related with or comes from organic compounds. If it is, then the Cl $2p_{3/2}$ peak binding energy at (200.5-202.5 eV)[25,26]. Cl $2p_{1/2}$ and $2p_{3/2}$, Pd $3d_{3/2}$ and $3d_{5/2}$ chemical shift for Cl and Cl^{-1}. Due to the weight of (8 gm) of hydroxide was enough to separate chlorine from the Palladium in presence of two factors, chemical represented by the presence of alcohol and water, and the second is physical represented by heat and pressure. A strong signal from Pd($3d_{5/2}$) is detected as a spin orbit doublet deconvolution of the XPS Pd3d peak in at (338.93 and 338.03 eV) with total amount (1.03 and 3.74 At%) for the product of MWCNTs and TiO_2/Pd/MWCNTs composite respectively. Where the catalyst formation of palladium hydroxide takes place on the surface of carbon and a chemical binding such as Pd–C–O can be formed at the interface between Pd and $C_2H_5O^-$ during the consequent calcination and reduction steps as in TiO_2/Pd/MWCNTs composite material. Deconvolution of the XPS Ti $2p_{3/2}$ peak in figure (9) has a binding energy of (458.8 eV), with total amount (13.34 At%)which is characteristic of Ti^{4+} present in TiO_2. As the amount of deposited metal increases, the Ti $2p_{3/2}$ peak evolves into a broad structure due to the presence of Ti in different chemical environments [26,27]. The XPS results indicate that MWCNTs prepared with palladium catalysts synthesized by hydrothermal technique retain chlorine on its surface.

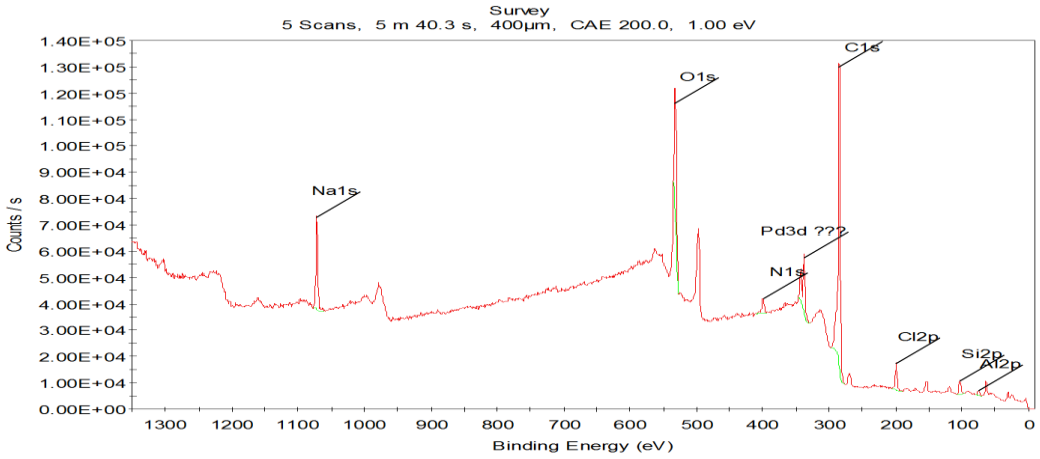

Figure (8) Schematic of XPS survey peaks deconvolution of MWCNTs and the assigned bonds.

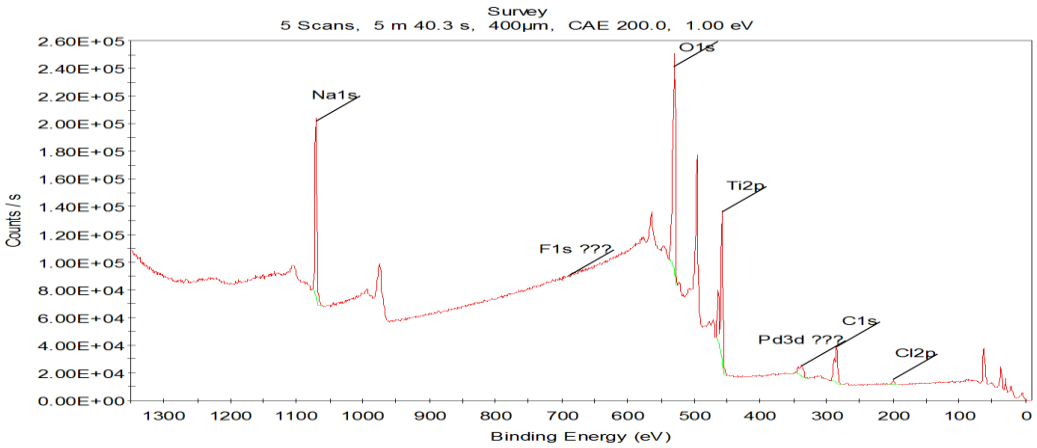

Figure (9) Schematic of XPS survey peaks deconvolution of TiO_2 /Pd MWCNTs and the assigned bonds.

UV-Visible absorption spectra of the product of MWCNTs and TiO_2/Pd/MWCNTs composite are illustrated in figure (10). An enhancement of absorption can be showed for TiO_2/Pd/MWCNTs composite material. The absorption band observed at around 292 nm can be referred to the pure MWCNTs. This absorption is feature of sprinkled MWCNTs, whereas hardly bunched CNTs show a different absorption edge. So, the salience of exceedingly sprinkled MWCNTs in the Ethanol Alchohol makes it possifor the molecular TiO_2 precursor to access the bare surface of the MWCNTs for disintegration and submissive TiO_2 formation.

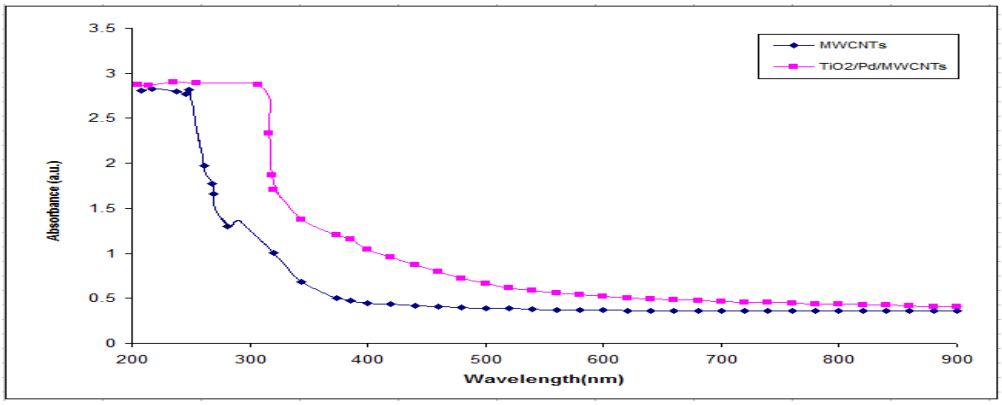

Figure (10) UV-Visible absorption spectra of the product of MWCNTs and TiO_2/Pd/MWCNTs composite.

A significant shift toward visible region in the spectral photoresponse more than 500 nm in little bit is observed for TiO_2/Pd/MWCNTs. Also the absorption spectrum shows scattering in the range 370–292 nm range due to formation nanoclusters of MWCNTs in the TiO_2 matrix[28,29].

Current-Voltage Characteristics Measurements at Dark and Illumination

Initially, manufacturing process of a TiO_2/Pd/MWCNTs:n-Si solar cell including create a cell device window by transferring a MWCNTs film on a n-Si wafer and putting Ag paste on the film, making grooves away the MWCNTs layer to form direct MWCNTs:n-Si junction, incrustation a thin TiO_2/Pd/MWCNTs film on top side of the wafer as antireflection layer using the Technique of Pulsed Laser Deposition , and chemically doping of the cell by spraying HF acid. Two cells was worked by pursue previous procedure to manufacture two cells, first one MWCNTs:n-Si and the second one TiO_2/Pd/MWCNTs:n-Si as in figure (11), illustrate the basic diagram of solar cell junction[30,31].

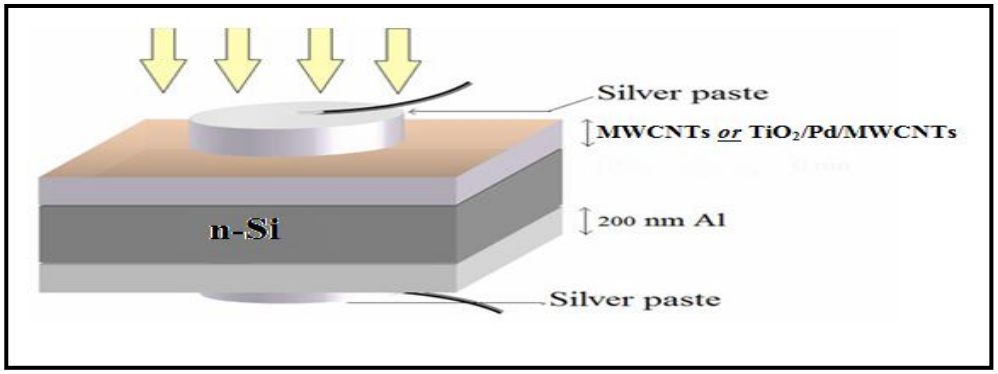

Figure (11) the basic diagram of solar cell junction.

The (I-V) characteristic in the thin films at dark is considered one of the most important parameter of devices measurements; as a tool for analyzing the behavior of

the current with the applied forward and reverse bias voltage. Figure (12) shows I-V characteristics for MWCNTs-Si and TiO_2/Pd/MWCNTs:n-Si heterojunction under dark for forward and reverse bias voltages. The curve exhibit in this figure a highly non-linear behavior and this is an indication of the conduction mechanism as non-ohmic in nature. It is clear that , in the forward direction of the diode , the current flows relatively freely while in the reverse direction. As the majority and minority carrier concentration is higher than the intrinsic carrier concentration which generate the recombination current at the low voltage region (0-0.3) Volt, because of the excitation of electrons from valence band (V.B) to conduction band (C.B) that will recombine them with the holes which are found at the V.B., and this is observed by the little increase in recombination current at low voltage region (0-0.3)Volt , while the tunneling current occurs at the high voltage region. After that , there is a fast exponential increase in the current magnitude with increasing of the voltage and this is called diffusion current, which dominates at high voltage (> 0.3 Volt). In the reverse bias region , the bias voltage leads to increase the width of the depletion layer which leads to decrease in the majority and minority carriers concentration and being lower than the intrinsic carriers concentration. The reverse bias current also contains two regions. In the first region of low voltages (< 0.1 Volt), the current slightly increases with increasing of the applied voltage, and the generation current dominates, while at the second high voltage region (> 0.1 Volt), the diffusion current dominates.

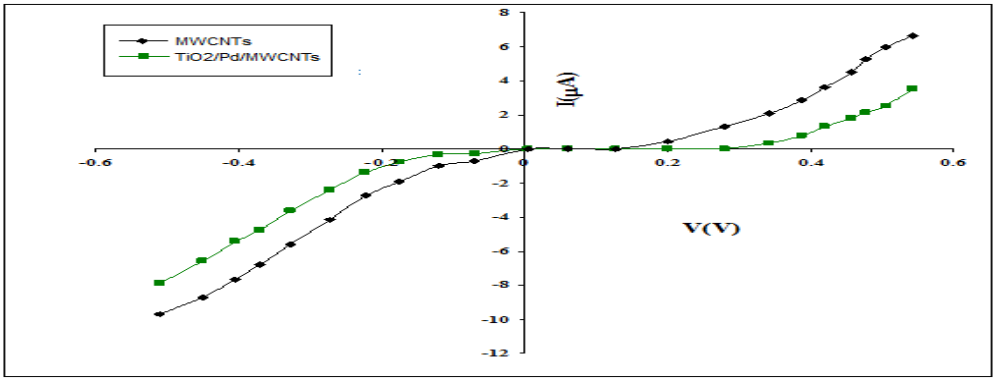

Figure (12) I-V characteristics under dark for MWCNTs-Si and TiO_2/Pd/MWCNTs:n-Si Heterojunction.

The relation between illumination current and voltage of the MWCNTs:n-Si and TiO_2/Pd/MWCNTs:n-Si heterojunctions prepared were presented in Figure (13). The measurements were carried out under illumination with power density equal to (105) mW/cm^2, where illuminated cell area is (1*1 cm^2). These curves illustrate the behavior of the photocurrent with the forward and reverse bias .

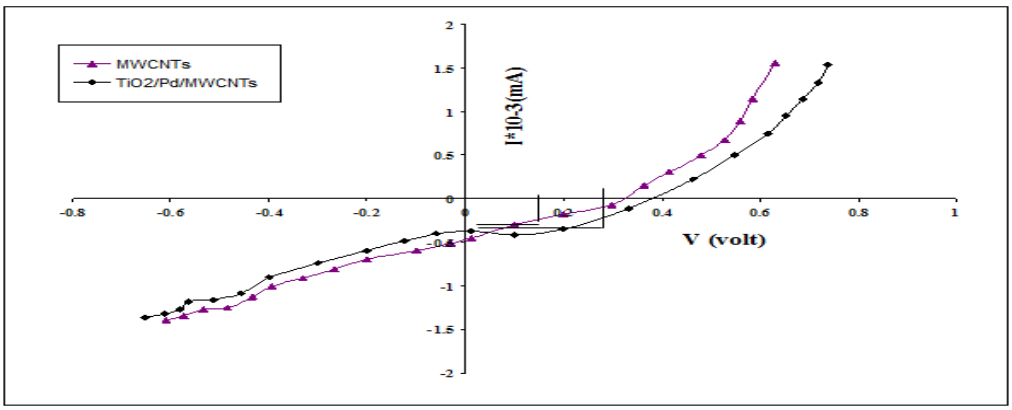

Figure (13) I-V characteristics for MWCNTs:n-Si and TiO_2/Pd/MWCNTs:n-Si heterojunctions under illumination by 105mW/cm^2 white light

Voltage. From this figure it is clear that the photocurrent increases with increasing of the bias voltage. These results can be interpreted as, with increasing the incident power density the free carrier hall density is increased, and the trap depth is decreased. At forward biasing voltage the current rises exponentially with forward voltage until the slope becomes more gradual. This can be due to high level injection of carriers such that the applied voltage is no longer totally developed across the depletion region. This may be due to the defect in the interface states. I_{sc} and V_{oc} are the short circuit current and the open circuit voltage and I_m and V_m are the current and

voltage corresponding to the maximum power point. This is the point where maximum power can be generated by the device.
Another parameter of interest is the Fill factor (F.F) given by the relation.

$$F.F=V_mI_m/V_{oc}I_{sc} \quad \text{.....(1)}$$

The photovoltaic conversion efficiency is another important parameter. It is a measure of the amount of light energy that is converted into electrical energy and is given by:

$$\eta=P_m/P_{in}=F.F\times I_{sc}\times V_{oc}/P_{in} \times 100\% \quad \text{...(2)}$$

Where:
P_m is the area of the maximum power rectangle, and P_{in} is the incident power.
The values of I-V parameters (V_{oc} , I_{sc} , V_{max} , I_{max} , F.F and η) were tabulated in Table (1). In general it can be observed that, the I_{sc} increases as the MWCNTs content (if the content is changeable) increases and power intensity increases. This may be due to the defect in the interface state. The fill factors of the devices for two types were in range of (30-43%) [31,32].

Table (1) I-V parameters for MWCNTs-Si and TiO_2/Pd/MWCNTs- Si heterojunctions illuminated by 105 mW/cm^2 white light.

Material of Cell	V_{oc} (V)	$I_{sc}*10^{-3}$ (mA)	V_m (V)	I_m*10^{-3} (mA)	FF	η
MWCNTs	0.30	48	0.185	24	0.31	7.16
TiO_2/Pd/MWCNTs	0. 37	43	0.23	30	0.43	10.52

Conclusion

Low-temperature hydrothermal track has been successfully developed to synthesize MWCNTs and CNSs at (190 ºC) with catalyst $PdCl_2$ and the carbon source using PEG, then the diameters of MWCNTs prepared are small this method. Which could generate a considerable amount of multi-walled carbon nanotubes and Carbon Nano-Sheets for the subsequent hydrothermal growth. Because TiO_2 nanoparticles were directly deposited on MWCNTs, electronic interaction might exist between TiO_2 and MWCNTs as revealed in some semiconducting nanoparticle-CNT hybrid systems. If electron transfer from the TiO_2 nanoparticles to MWCNTs occurs under light excitation, the current flow through the device should change accordingly and even 1% increase of efficiency is critical for pushing forward practical applications and sometimes requires substantial modification or improvement of current cell structures.

References

[1] P. Poncharal, Z.L. Wang, D.Ugarte, W.A.D.Heer, "Electrostatic deflections and electromechanical resonances of carbon nanotubes.", Science, Vol. 283, No.5407, p.p. 1513–1519, 1999.

[2] S. Iijima , "Helical microtubes of graphitic carbon.", Nature, Vol. 354, No. 6348, p.p. 56–64, 1991.

[3] C.D. Scott, S.Arepalli, P.Nikolaev, R.E.Smalley, "Growth mechanism for single-wall carbon nanotubes in a laser ablation process.", Appl Phys A, Vol. 72, No.5, p.p. 573-580, 2001.

[4] D.S. Bethune, G.H.Kiang, M.S.Devries, G.Gorman, R.Savoy, J. Vazquez, et al., "Cobalt-catalysed growth of carbon nanotubes with single-atomic-layer walls.", Nature, Vol.363, No.6430, p.p. 605-612, 1993.

[5] B.W. Smith, M.Monthioux, D.E. Luzzi, "Encapsulated C60 in carbon nanotubes.", Nature, Vol. 396, No. 6709, p.p. 323-324, 1998.

[6] J.M. Calderon-Moreno, M.Yoshimura, "Hydrothermal processing of high-quality multiwall nano tubes from amorphous carbon.", Journal of American. Chemistry Society, Vol. 123, No. 4, p.p.741–743, 2001.

[7] K.V. Jason, J.B. Jonathan, E.R. Jeffery, E.B. Allan, L.W. Geoffrey, D.F. Bradly,"Low-temperature growth of carbon nanotubes from the catalytic decomposition of carbon tetrachloride.", Journal of American Chemical Society, Vol.126, No. 32, p.p. 9936-9937, 2004.

[8] A. Celzard, J.F.Mareche, G.Furdin, "Surface area of compressed expanded graphite.", Carbon, Vol.40, No. 14, p.p. 2713-2718, 2002.

[9] A. V.Melechko, Merkulov V. I., McKnight T. E., Guillorn M. A., Klein K. L., Lowndes D. H. and M. L. Simpson, "Vertically aligned carbon nanofibers and related structures: Controlled synthesis and directed assembly.", Journal of Applied Physics, Vol. 97, No. 041301, p.p. 1-39, 2005.
[10] Claes-Henrik Anderson, "Chemistry of Carbon Nanostructures: Functionalization of Carbon Nanotubes and Synthesis of Organometallic Fullerene Derivatives.", Uppsala Universitet, Sweden, 2011.
[11] P. Poncharal, C. Berge, Y. Yi, Z. L. Wang, and W. d. Heer, "Room temperature ballistic conduction in carbon nanotubes.", Journal of Physical Chemistry B, Vol. 106, No. 47, p.p. 12104-12118, 2002.
[12] P.J. Harris," Carbon nanotubes and other graphite structures as contaminants on evaporated carbon films.", Journal of Microscopy, Vol. 186, No. 1, p.p. 88-90 1997.
[13] C. Ducati, L. Alexandrou, M. Chhowalla, G. Amaratunga, and J. Robertson," Temperature selective growth of carbon nanotubes by Chemical Vapor Deposition.", Journal of Applied Physics, Vol. 92, No. 6, p.p. 3299–3306, 2002.
[14] J. Tersoff and R. S. Ruoff, "Structural properties of a carbon-nanotube crystal.", Physical ReviewLetters, Vol. 73, No. 5, p.p. 676-679, 1994.
[15] N. Wang, Z. K. Tang, G. D. Li, and J. S. Chen, "Single-walled 4Å carbon nanotube arrays.", Nature, Vol.408, No. 6808, p.p. 50-51, 2000.
[16] B. Bhushan, "Springer: Handbook of Nanotechnology.", Springer – Verlag, 2004.
[17] H. Cui, D. Palmer, O. Zhou, and B. R. Stoner, "Aligned carbon nanotubes via microwave plasma enhanced chemical vapor deposition.", presented at MRS Fall Meeting, Boston, 1999.
[18] Wenzhong Wang, J.Y. Huang, D.Z. Wang and Z.F. Ren," Low-temperature hydrothermal synthesis of multiwall carbon nanotubes.", Letters to the Editor, Carbon, Vol. 43, No. 6, p.p. 1328-1331, 2005.
[19] nanotubes", Department of Physics, Boston College, USA, Carbon, 2005, 43, 1317–1339. Lewis, N. S. Toward cost-effective solar energy use. Science 315, 798–801, 2007.
[20] Gra¨tzel, M.,"Photoelectrochemical cells.", Nature, Vol. 414, No. 6861, p.p. 338–344, 2001.
[21] Yongye Liang, Zheng Xu, Jiangbin Xia, Szu-Ting Tsai, Yue Wu, Gang Li, Claire Ray and Luping Yu," For the Bright Future-Bulk Heterojunction Polymer Solar Cells with Power Conversion Efficiency of 7.4%.", Journal Of Advanced Materials, Vol. 22, No. 20, p.p. E135-E138, 2010.
[22] Yanming Sun, Gregory C. Welch, Wei Lin Leong, Christopher J. Takacs, Guillermo C. Bazan and Alan J. Heeger," Solution-processed small-molecule solar cells with 6.7% efficiency.", Nature Materials, Vol. 11, No. 160, p.p. 44-48, 2012.
[23] C.Albert Thompson, " X-RAY DATA BOOKLET", Book, Center for X-Ray Optics Advanced Light Source.", Lawrence Berkeley National Laboratory, 94720, USA, Second Edition, 2001.
[24] B. Vincent Crist, "Handbook of Monochromatic XPS Spectra, Polymers and Polymers Damaged by X-Rays.", Book, John Wiley & Sons, Second edition,2000.
[25] T.I.T. Okpalugo, P. Papakonstantinou, H. Murphy, J. McLaughlin and N.M.D. Brown, "High resolution XPS characterization of chemical functionalized MWCNTs and SWMWCNTs.", Journal of Carbon, Vol. 43, No. 1, p.p. 153-161, 2005.

[26] V. Datsyuk, M. Kalyva, K. Papagelis, J. Parthenios, D. Tasis, A. Siokou, I. Kallitsis, C. Galiotis, "Chemical oxidation of multiwalled carbon nanotubes.", Science Direct, J. of Carbon, Vol. 43, No. 8, p.p. 833-840, 2008.

[27] Alexandre Felten, Irene Suarez-Martinez, Xiaoxing Ke, Gustaaf Van Tendeloo, Jacques Ghijsen, Jean-Jacques Pireaux, Wolgang Drube, Carla Bittencourt and Christopher P. Ewels, "The Interface between Titanium and Carbon Nanotubes.", Journal of ChemPhysChem, Vol. 10, No. 11, p.p. 1799-1804, 2009.

[28] Yun Ye, Shoujin Cai, Min Yan, Tianyuan Chen, Tailiang Guo, " Concentration detection of carbon nanotubes in electrophoretic suspension with UV–Vis. spectrophotometry for application in field emission devices.", College of Physics and Information Engineering, Fuzhou University, China, ELSEVIER Pub., J. of Applied Surface Science, Vol. 284, No. 7, p.p. 107-112, 2013.

[29] S.Sawanta Mali, A.Chirayath Betty, N. Popatrao Bhosale, and P. S.Patil, " Synthesis, Characterization of Hydrothermally Grown MWCNT–TiO_2 Photoelectrodes and Their Visible Light Absorption Properties.", Thin Film Materials Lab., Dept. of Physics, Shivaji University, Kolhapur, India, The Electrochemical Society, ECS Journal of Solid State Science and Technology, Vol. 1, No. 2, p.p. 15-23, 2012.

[30] Jinquan Wei, Yi Jia, Qinke Shu, Zhiyi Gu, Kunlin Wang, Daming Zhuang, Gong Zhang, Zhicheng Wang, Jianbin Luo, Anyuan Cao, and Dehai Wu,"Double-Walled Carbon Nanotube Solar Cells.", Journal of Nano Letters, Vol.7, No.8, p.p. 2317-2321, 2007.

[31] Enzheng Shi,Luhui Zhang, Zhen Li, Peixu Li, Yuanyuan Shang, Yi Jia, Jinquan Wei, Kunlin Wang, Hongwei Zhu, Dehai Wu, Sen Zhang, and Anyuan Cao," TiO_2-Coated Carbon Nanotube-Silicon Solar Cells with Efficiency of 15%.", Journal of Scientific Reports, Vol. 2, No. 884, p.p. 1-5, 2012.

[32] Xiaochang Miao, Sefaattin Tongay, Maureen K. Petterson, Kara Berke, Andrew G. Rinzler, Bill R. Appleton, and Arthur F. Hebard," High Efficiency Graphene Solar Cells by Chemical Doping.", American Chemical Society Pub., Journal of Nano Letters, Vol. 12, No. 1021, p.p. 2745-2750, 2012.